RSC Medicinal Chemistry

Accepted Manuscript

This article can be cited before page numbers have been issued, to do this please use: D. Miller, S. A. Voell, I. Sosi, M. Proj, O. Rossanese, G. Schnakenburg, M. Gütschow, I. Collins and C. Steinebach, *RSC Med. Chem.*, 2022, DOI: 10.1039/D2MD00064D.

ROYAL SOCIETY OF CHEMISTRY

rsc.li/medchem

RSC Medicinal Chemistry

View Article Online
DOI: 10.1039/D2MD00064D

COMMUNICATION

Encoding BRAF Inhibitor Functions in Protein Degraders

Daniel S. J. Miller,[a] Sabine A. Voell,[b] Izidor Sosič,[c] Matic Proj,[c] Olivia W. Rossanese,[a] Gregor Schnakenburg,[d] Michael Gütschow,[b] Ian Collins,[a] and Christian Steinebach *,[b]

Received 00th January 2022,
Accepted 00th January 2022

DOI: 10.1039/x0xx00000x

Various BRAF kinase inhibitors were developed to treat cancers carrying the BRAF^{V600E} mutation. First-generation BRAF inhibitors could lead to paradoxical activation of the MAPK pathway, limiting their clinical usefulness. Here, we show the development of two series of BRAF^{V600E}-targeting PROTACs and demonstrate that the exchange of the inhibitor scaffold from vemurafenib to paradox-breaker ligands resulted in BRAF^{V600E} degraders that did not cause paradoxical ERK activation.

Introduction

Kinases catalyse phosphorylation reactions of target substrates, which is key to control intra- and extracellular signalling pathways. Dysregulation of these enzymes can lead to enhanced cellular proliferation and contribute to cancer growth. In particular, regulatory disturbance of the mitogen-activated protein kinases/extracellular signal-regulated kinases (MAPK/ERK) axis is frequently observed in cancer. Accordingly, kinase inhibitors directed against the ERK signalling pathway received considerable attention in drug discovery.[1,2] One compound class was developed to target BRAF harbouring a point mutation at position 600 (BRAF^{V600E}), the most prevalent oncogenic protein mutation, and a critical driver of malignant melanoma. This modification enhances spontaneous RAF homo- and heterodimerisation leading to the uncontrolled activity of the kinase.[3] BRAF inhibitor (BRAFi) research enjoyed vast success and culminated in several generations of RAF inhibitors, including clinically approved drugs such as vemurafenib (PLX4032) and dabrafenib (Figure 1A).[4–6] However, initial accomplishments were mitigated by the rapid development of drug resistance and most melanoma patients relapse within a short time.[4] Surprisingly, these BRAFi did not inhibit ERK signalling in tumours possessing additional mutations in RAS or its upstream signalling receptors.[7] BRAF^{V600E} inhibitors such as vemurafenib fail to prevent BRAF-CRAF heterodimers.[4,8] As RAF dimerization and activation is allosterically regulated, one inhibitor-bound protomer can still transactivate the other component of a heterodimer and induce proliferative MAPK signalling, thus promoting paradoxical ERK activation.[9]

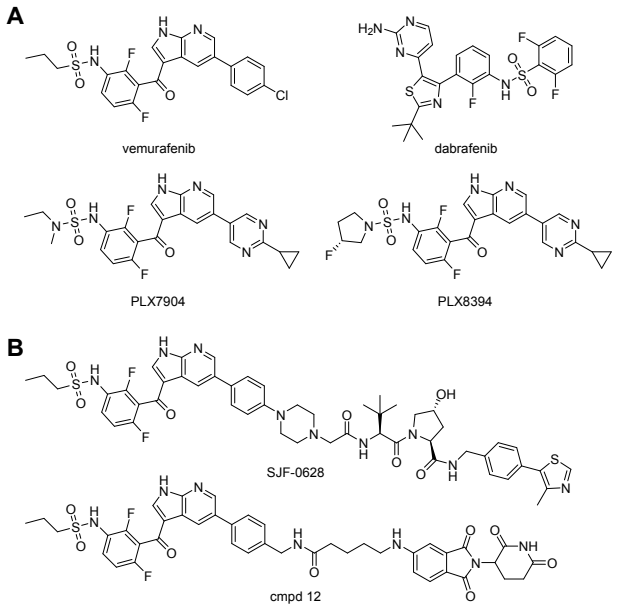

Fig. 1 (A) Structures of the clinically approved BRAF^{V600E} inhibitors vemurafenib (PLX4720) and dabrafenib as well as paradox-breakers PLX7904 and PLX8394. (B) Selected BRAF-targeting PROTACs.

To overcome the issues associated with paradoxical activation, further development of drugs that inhibit BRAF and evade resistance mechanisms is needed. Next-generation BRAF^{V600E} inhibitors PLX7904 and PLX8394 (Figure 1A) were aimed at restricting RAF dimerisation *via* shifting critical amino acid side chains located at the interface responsible for dimer formation (Figure 2).[7,10] An alternative approach is focused at depleting kinases at the proteome level by applying the proteolysis-

[a] *Cancer Research UK Cancer Therapeutics Unit at The Institute of Cancer Research, London SW7 3RP, United Kingdom.*
[b] *Pharmaceutical Institute, Pharmaceutical & Medicinal Chemistry, University of Bonn, D-53121 Bonn, Germany.*
[c] *Faculty of Pharmacy, University of Ljubljana, SI-1000 Ljubljana, Slovenia.*
[d] *Institute of Inorganic Chemistry, University of Bonn, D-53121 Bonn, Germany*

† Electronic Supplementary Information (ESI) available: Supplementary Table 1, Supplementary Figures S1-S9; biological, chemical and physicochemical methods; synthetic procedures; structures, ^{1}H NMR, ^{13}C NMR and MS data; Western blots. See DOI: 10.1039/x0xx00000x

View Article Online
DOI: 10.1039/D2MD00064D

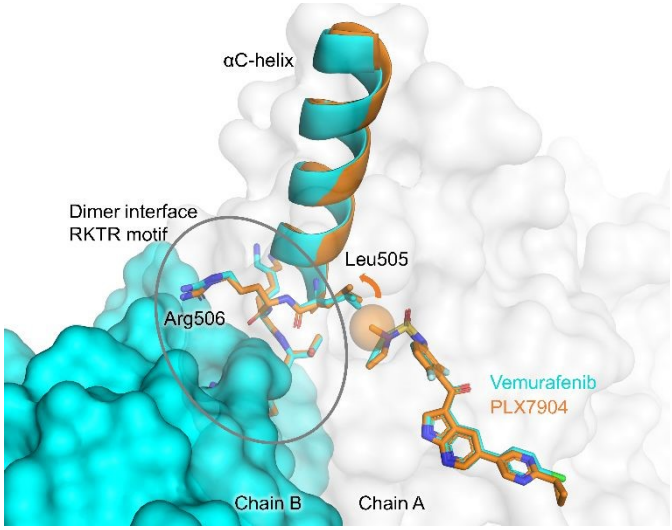

Fig. 2 BRAF^{V600E} in complex with vemurafenib (cyan, PDB 3OG7) and PLX7904 (orange, PDB 4XV1). The surface of the *N*-methyl group of PLX7904 illustrates the reason for the Leu505 shift, which affects the conformation of the conserved RKTR motif (shown with sticks) at the dimer interface. Arg506 is particularly important for the stabilization of dimeric complexes. In the case of binding of a paradox-breaker, Arg506 in the αC helix displays an outward movement which reduces the transactivation of ERK signalling. The protein surface of chains A and B is shown for 3OG7 only.

targeting chimeras (PROTACs) technique.[11–13] In this new modality, chimeric degrader molecules induce the destruction of target proteins by modulating the substrate scope of E3 ligases through ternary PROTAC : E3 : target complexes. The ligase-mediated ubiquitination of proteins of interest can ultimately induce their degradation *via* the proteasome machinery.[14–16] Multiple teams have attempted to degrade BRAF proteins using degraders derived from rigosertib,[17] dabrafenib,[18] vemurafenib,[19,20] or other RAF inhibitors.[18] A selection of vemurafenib-based PROTACs are shown in Figure 1B. Kinase degraders may have intrinsic advantages over classical inhibitors as they silence both catalytic and non-catalytic functions of BRAF. However, PROTAC response may depend on the RAS/RAF mutational context,[12] as well as the expression levels of the hijacked E3 ligase.[21] Furthermore, the so-called "hook effect"[14] could lead to disadvantageous features of BRAF^{V600E} PROTACs and stimulate RAF dimerisation when productive ternary complexes are prevented.[22]

In this study, we designed a series of von Hippel-Lindau (VHL)-based PROTACs targeting BRAF^{V600E} *via* PLX-derived ligands. Particular attention was paid to the BRAFi functions of the bivalent molecules. Addressing the paradoxical activation in a particular mutational context, we demonstrate an advantageous feature of these PROTACs, which arises from the introduction of next-generation paradox-breaker ligands. Such a conceptual approach may lead to a more effective generation of BRAF^{V600E}-targeting PROTACs.

Results and discussion

Vemurafenib was selected as the BRAF^{V600E} binding moiety to design bifunctional degrader molecules. Visual inspection of crystal structures of BRAF^{V600E} in complex with vemurafenib (PDB 3OG7) or with a homodimeric derivative (PDB 5JT2)[26] revealed the phenyl ring at the azaindole to be solvent-exposed and suitable for linker attachment (Figure S1). To exploit this exit vector for PROTAC design, synthetic access to a modified vemurafenib scaffold was necessary. Key intermediate **3** (Scheme 1) was synthesised from the acid **1** and 5-bromo-7-azaindole (**2**) by an optimised Friedel-Crafts acylation procedure (Table S1). The synthetic entry deviated from the initially published route.[27] The correct structure of the acyl product **3** was confirmed by means of NMR spectroscopy and X-ray crystallography (Figure S2).[28] Its subsequent transformation in microwave-assisted Suzuki cross-couplings afforded vemurafenib (**4**) and functionalised BRAF^{V600E} inhibitors **5**–**7**. An indirect access to **8** *via* the aldehyde **7** and subsequent reductive amination proceeded in significant better yields compared to the direct use of the appropriate boronic acid leading to **8** from **3**.

VHL-binding E3 ligase ligands were readily available as described in our recent work on the improved synthetic pathway towards the amine **9** and the phenolic derivative **10**.[29] Notably, these distinct functional groups allowed the installation of orthogonally protected linkers **11** and **12**[30,31] on two differently oriented exit vectors of the E3 ligands.

For the first series of VHL-based PROTACs, the Cbz protecting group of linkers **11** was removed hydrogenolytically, and the amine group was coupled to the carboxyl group released from **6**. The so obtained vemurafenib-linker conjugates were deprotected at the terminal linker moiety and subjected to a further amide formation with VHL ligand **9**. The final PROTACs **15a** to **15c** cover a moderate range of lipophilicity (Table 1)

Table 1 Overview on physicochemical properties as well as kinase inhibition and degradation potencies of BRAF^{V600E}-targeting PROTACs.

Cmpd	Linker atoms	TPSA[a]	elogD[b]	%PPB[c]	IC_{50}[d] (nM)	D_{BRAF}[e]
GW5074	--	49	2.3	n.d.[f]	5.8	n.d.
15a	10	288	2.3	95%	8.5	>95%
15b	16	297	2.4	95%	0.31	>95%
15c	20	288	3.7	96%	48	>95%
16a	17	288	3.6	96%	10	77%
16b	13	297	2.5	96%	3.4	73%
16c	16	297	2.7	96%	3.8	77%

[a] Topological polar surface area given in Å². [b] Experimental distribution coefficient at *p*H 7.4.[23] [c] Protein binding values were estimated by an HPLC-based method.[24] [d] *In vitro* BRAF^{V600E} inhibition employing a radiometric assay using 10 µM [^{33}P]-ATP and 1 µM substrate peptide,[25] see also Figure S8. [e] Degradation indicated as remaining BRAF^{V600E} levels after 4 h treatment with 1 µM of each compound (as determined by densitometric analysis of Western blot assays). [f] Not determined.

View Article Online
DOI: 10.1039/D2MD00061D

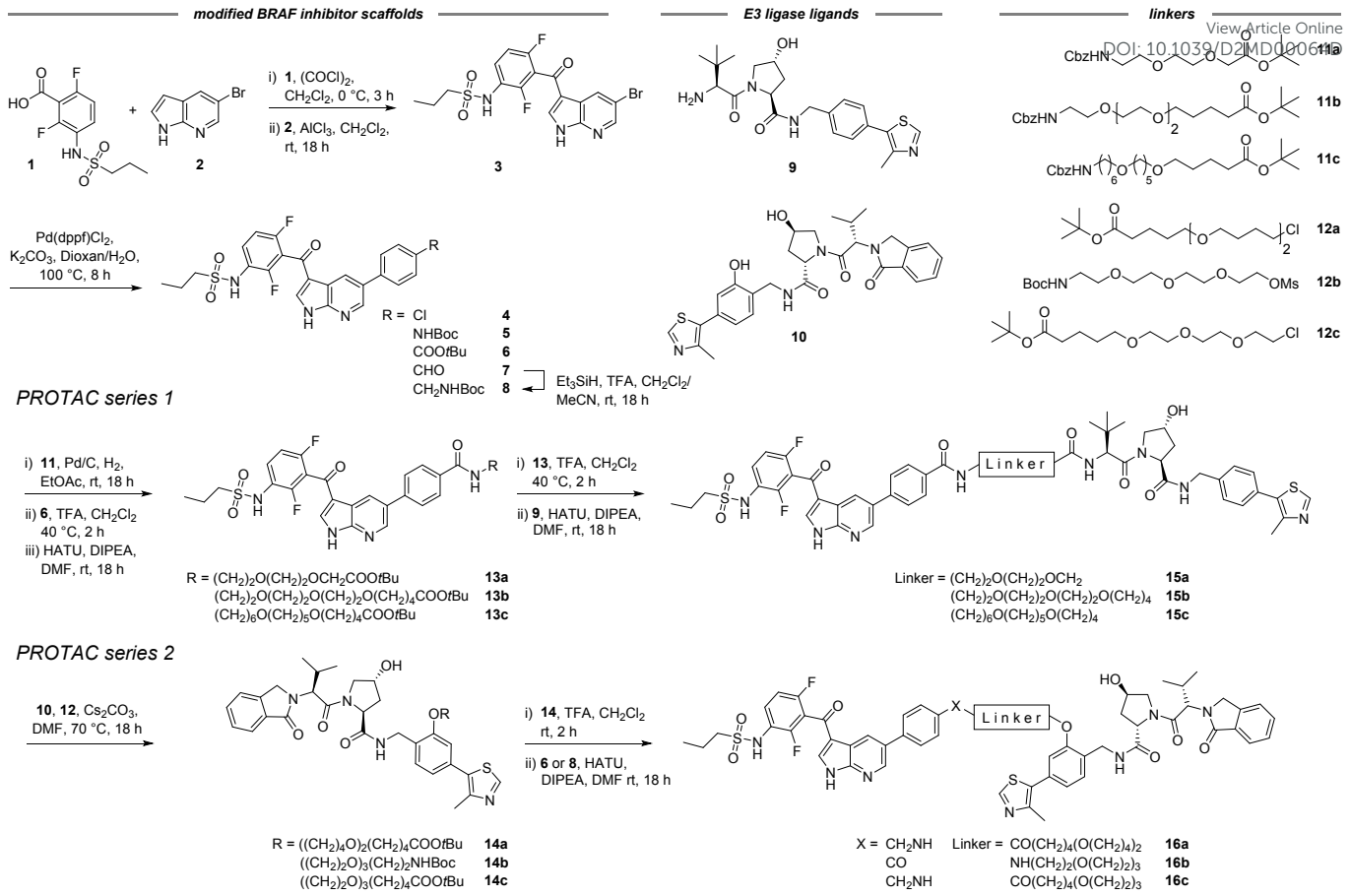

Scheme 1 Modular design and synthesis of vemurafenib-derived BRAF^{V600E} PROTACs.

and span linker lengths between 10 and 20 atoms. In the second series of PROTACs, the linker was tethered to the VHL ligand by alkylating the phenolic group in **10**. The protecting groups at the VHL-linker conjugates **14** were removed, and intermediates were coupled to **6** or **8** after their respective deprotection. In PROTACs **16a–16c**, which represent differently oriented VHL-based degraders, lipophilicity and linker length fall into a similar range as in the first series.

Next, we investigated our set of putative BRAF^{V600E} degraders in an *in vitro* BRAF inhibition assay. The RAF inhibitor GW5074 was used as a control.[32] All compounds retained BRAF mutant inhibitory properties, but apparent differences were observed within the two subseries (Table 1). Surprisingly, compounds **15c** and **16a,** possessing the most extended and hydrophobic linkers, had the highest IC_{50} values. Compounds were then tested in SK-MEL-28 cells (BRAF^{V600E}/NRAS^{wt}) for their ability to induce RAF degradation. After a short treatment time of 4 h and concentrations between 0.1 and 10 µM, all compounds significantly reduced phospho-ERK (p-ERK) levels, but only compounds **16** caused moderate target degradation (Figure S3 and Table 1). However, prolonged treatment with 10 µM of the PROTACs did not result in more efficient BRAF^{V600E} degradation (Figure S4). Given these *in vitro* and *in cellulo* features, it is likely that the compounds did not efficiently form ternary complexes needed for the ubiquitination step of the PROTAC's mode of action. In line with this, the recently described BRAF degraders SJF-0628 and cmpd 12 (Figure 1B) contain considerably shorter linkers, underscoring the potential need for positive cooperativity to efficiently degrade BRAF.[33]

For comparison, the established BRAF PROTACs SJF-0628 and cmpd 12 were included in our studies.[19,20] The BRAF^{V600E} degrader SJF-0628 caused significant degradation of its target protein in SK-MEL-28 cells (Figure S5A) between 0.1 and 10 µM. As expected, the control compound SJF-0661, which is tailored to be inoperative at the VHL-binding unit, did not cause BRAF^{V600E} degradation. The CRBN-based PROTAC cmpd 12 caused only modest target degradation in our assay. All compounds provoked a fundamental reduction of pERK levels which may be attributed to either BRAF^{V600E} degradation or inhibition.

To pinpoint the encoding of kinase inhibitor functions in their derived degraders, we adapted the privileged linker design in SJF-0628 for the syntheses of paradox-breaker PROTACs (Scheme 2). Their synthetic entry proceeded *via* the nitro derivative **18,** which was subsequently reduced to **19**. Sulfamoylation with *N*-ethyl-*N*-methylsulfamoyl chloride gave azaindole **20,** which was further subjected to Suzuki cross-coupling reactions with appropriate boronic acid pinacol esters. Products **21** and **22** represent close analogues of the paradox-breakers PLX7683 and PLX7904, respectively.[7] However, the solvent-exposed aryl moieties were substituted

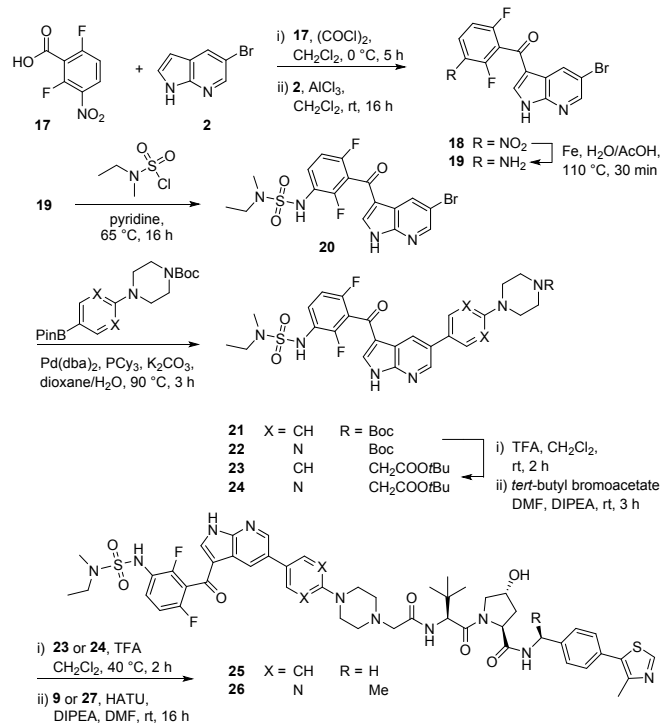

Scheme 2 Synthesis of PROTACs possessing paradox-breaker properties.

with an *N*-Boc-piperazine heterocycle to install a linker handle. Subsequent alkylation with *tert*-butyl bromoacetate and coupling to the VHL ligands **10** or **27** yielded putative paradox-breaking PROTACs **25** and **26**. The latter bears an additional, stereochemically defined methyl group at the VHL ligand, which was reported to enhance degrader efficacy.[23,34] This modification balanced the physicochemical properties of **26** (Table 2). However, the polar surface area is increased due to the pyrimidine moiety present in this BRAFi ligand.

Degraders **25** and **26** were then tested in SK-MEL-28 cells for BRAF^{V600E} degradation (Figure S5B). Surprisingly, only **25**

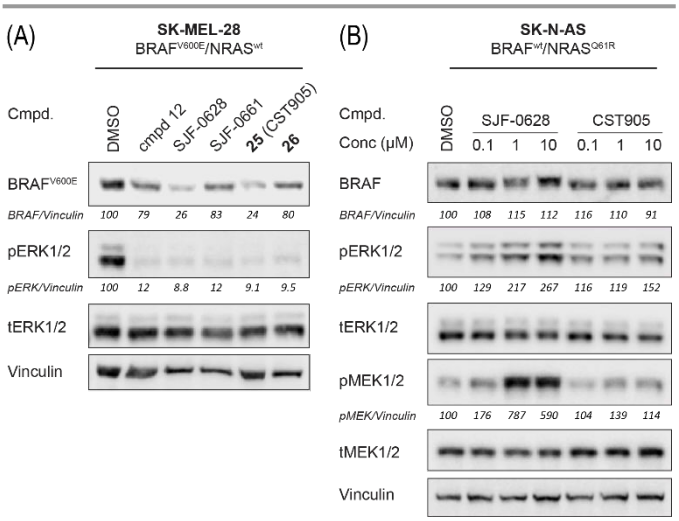

Fig. 3 (A) Head-to-head comparison of vemurafenib-based PROTACs (cmpd 12, SJF-0628), the negative control SJF-0661 with paradox-breaker PROTACs **25** and **26**. SK-MEL-28 cells were treated with 10 µM compounds for 24 h; (B) In the NRAS mutant cell line SK-N-AS, SJF-0628 but not **25** (CST905) induced paradoxical ERK-signalling. Cells were treated for 4 h at the dose indicated. Quantified values for BRAF^{V600E}, pERK1/2, and pMEK1/2 refer to mean of duplicates.

Table 2 Overview on physicochemical properties as well as BRAF^{V600E} degradation potencies of a PLX4032-based PROTAC and paradox-breaking PROTACs **25** and **26**.

View Article Online
DOI: 10.1039/D2MD00064D

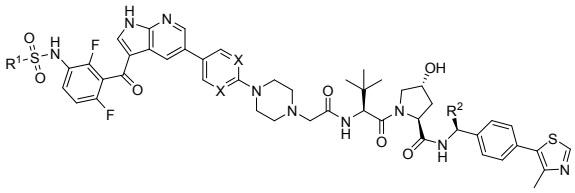

Cmpd	R^1	R^2	X	TPSA[a]	elogD[b]	%PPB[c]	D_{BRAF}[d]
SJF-0628		H	CH	247	2.9	96%	46%
25 (CST905)		H	CH	250	3.2	96%	52%
26		Me	N	276	3.2	96%	>95%

[a] Topological polar surface area given in Å². [b] Experimental distribution coefficient at *p*H 7.4.[23] [c] Protein binding values were estimated by an HPLC-based method.[24] [d] Degradation indicated as remaining BRAF^{V600E} levels after 4 h treatment with 1 µM of each compound (as determined by densitometric analysis of Western blot assays).

(CST905) showed distinct target degradation. Its effects on protein degradation (Figure 3A) and cell viability reduction (Figure S6) were comparable to SJF-0628 and significantly more pronounced compared to the control SJF-0661, which can only function as a BRAF^{V600E} inhibitor due to the mitigated ligase binding portion. Next, paradox-breakers **25** and **26** were investigated in the neuroblastoma cell line SK-N-AS possessing RAF wildtype and RAS mutant status. As expected, neither wildtype RAF nor pERK levels were affected by these compounds (Figure S7). A head-to-head comparison with SJF-0628 in this cell line (Figure 3B) demonstrated the undesired paradoxical activation of ERK signalling induced by the vemurafenib-derived PROTAC SJF-0628. The paradox-breaking PROTAC **25**, also referred to as development compound CST905, remedied this undesired feature.

Conclusions

We disclosed a new series of BRAF^{V600E}-targeting PROTACs in which the replacement of vemurafenib by a paradox-breaking BRAF ligand caused substantially different cellular outcomes. Herein, we introduce CST905, an exceptionally potent BRAF^{V600E} degrader with a DC_{50} value of 18 nM and a maximal degradation concentration of 50 nM after a short treatment time of 4 h (Figure S8). In the BRAF^{V600E}/NRAS^{wt} cell line SK-MEL-28, CST905 significantly reduced ERK phosphorylation (IC_{50} = 31 nM), and did not lead to paradoxical MAPK activation in a RAS-mutant cell line. Dissociating BRAF^{V600E} depletion from paradoxical activation of MAPK pathway might lead to compounds with significantly more durable efficacy and with safer profile in comparison to first-generation BRAF inhibitors. Furthermore, this study pinpoints the need to track inhibitor functions of incorporated target ligands in PROTACs.

Author contributions

M.G. and C.S. designed the study; D.S.J.M., G.S., and C.S. performed experiments; S.A.V., I.S., and C.S. synthesised compounds. M.P. created computational illustrations. All authors analysed and interpreted data; O.W.R., M.G., I.C., and C.S. supervised the project; C.S. wrote the manuscript with contributions from all co-authors. All authors have approved the final article.

Conflicts of interest

There are no conflicts to declare.

Acknowledgements

We thank C. Ennenbach, Prof. A.C. Filippou, M. Schneider (University of Bonn, Bonn, Germany), and M. Frelih (University of Ljubljana, Ljubljana, Slovenia) for their support and technical assistance. D.S.J.M., O.R. and I.C. acknowledge funding from Cancer Research UK programme grant C309/11566, and from The Institute of Cancer Research. I.S. acknowledges support by the Slovenian Research Agency (ARRS, program P1-0208 and grant J1-2485).

Notes and references

1 F. M. Ferguson and N. S. Gray, *Nat. Rev. Drug. Discov.*, 2018, **17**, 353–377.
2 P. Cohen, D. Cross and P. A. Jänne, *Nat. Rev. Drug Discov.*, 2021, **20**, 551–569.
3 J. Pan, H. Zhou, S. Zhu, J. Huang, X. Zhao, H. Ding and Y. Pan, *Cancer Manag. Res.*, 2018, **10**, 2289–2301.
4 D. E. Durrant and D. K. Morrison, *Br. J. Cancer*, 2018, **118**, 3–8.
5 P. B. Chapman, A. Hauschild, C. Robert, J. B. Haanen, P. Ascierto, J. Larkin, R. Dummer, C. Garbe, A. Testori, M. Maio, D. Hogg, P. Lorigan, C. Lebbe, T. Jouary, D. Schadendorf, A. Ribas, S. J. O'Day, J. A. Sosman, J. M. Kirkwood, A. M. M. Eggermont, B. Dreno, K. Nolop, J. Li, B. Nelson, J. Hou, R. J. Lee, K. T. Flaherty and G. A. McArthur, *N. Engl. J. Med.*, 2011, **364**, 2507–2516.
6 G. S. Falchook, G. V. Long, R. Kurzrock, K. B. Kim, T. H. Arkenau, M. P. Brown, O. Hamid, J. R. Infante, M. Millward, A. C. Pavlick, S. J. O'Day, S. C. Blackman, C. M. Curtis, P. Lebowitz, B. Ma, D. Ouellet and R. F. Kefford, *Lancet*, 2012, **379**, 1893–1901.
7 C. Zhang, W. Spevak, Y. Zhang, E. A. Burton, Y. Ma, G. Habets, J. Zhang, J. Lin, T. Ewing, B. Matusow, G. Tsang, A. Marimuthu, H. Cho, G. Wu, W. Wang, D. Fong, H. Nguyen, S. Shi, P. Womack, M. Nespi, R. Shellooe, H. Carias, B. Powell, E. Light, L. Sanftner, J. Walters, J. Tsai, B. L. West, G. Visor, H. Rezaei, P. S. Lin, K. Nolop, P. N. Ibrahim, P. Hirth and G. Bollag, *Nature*, 2015, **526**, 583–586.
8 B. Agianian and E. Gavathiotis, *J. Med. Chem.*, 2018, **61**, 5775–5793.
9 P. I. Poulikakos, C. Zhang, G. Bollag, K. M. Shokat and N. Rosen, *Nature*, 2010, **464**, 427–430.
10 Z. Karoulia, Y. Wu, T. A. Ahmed, Q. Xin, J. Bollard, C. Krepler, X. Wu, C. Zhang, G. Bollag, M. Herlyn, J. A. Fagin, A. Lujambio, E. Gavathiotis and P. I. Poulikakos, *Cancer Cell*, 2016, **30**, 485–498.
11 C. E. Grigglestone and K.-S. Yeung, *ACS Med. Chem. Lett.*, 2021, **12**, 1629–1632.
12 J. J. Feng and C. Zhang, *Nat. Chem. Biol.*, 2020, **16**, 1154–1155.
13 F. Yu, M. Cai, L. Shao and J. Zhang, *Front. Chem.*, 2021, **9**, 679120.
14 S.-L. Paiva and C. M. Crews, *Curr. Opin. Chem. Biol.*, 2019, **50**, 111–119.
15 Z. Hu and C. M. Crews, *ChemBioChem*, 2021, DOI:cbic.202100270.
16 T. Ishida and A. Ciulli, *SLAS Discov.*, 2020, **26**, 484–502.
17 H. Chen, F. Chen, S. Pei and S. Gou, *Bioorg. Chem.*, 2019, **87**, 191–199.
18 G. Posternak, X. Tang, P. Maisonneuve, T. Jin, H. Lavoie, S. Daou, S. Orlicky, T. Goullet de Rugy, L. Caldwell, K. Chan, A. Aman, M. Prakesch, G. Poda, P. Mader, C. Wong, S. Maier, J. Kitaygorodsky, B. Larsen, K. Colwill, Z. Yin, D. F. Ceccarelli, R. A. Batey, M. Taipale, I. Kurinov, D. Uehling, J. Wrana, D. Durocher, A.-C. Gingras, R. Al-Awar, M. Therrien and F. Sicheri, *Nat. Chem. Biol.*, 2020, **16**, 1170–1178.
19 X.-R. Han, L. Chen, Y. Wei, W. Yu, Y. Chen, C. Zhang, B. Jiao, T. Shi, L. Sun, C. Zhang, Y. Xu, M. R. Lee, Y. Luo, M. B. Plewe and J. Wang, *J. Med. Chem.*, 2020, **63**, 4069–4080.
20 S. Alabi, S. Jaime-Figueroa, Z. Yao, Y. Gao, J. Hines, K. T. G. Samarasinghe, L. Vogt, N. Rosen and C. M. Crews, *Nat. Commun.*, 2021, **12**, 920.
21 J. Wei, F. Meng, K.-S. Park, H. Yim, J. Velez, P. Kumar, L. Wang, L. Xie, H. Chen, Y. Shen, E. Teichman, D. Li, G. G. Wang, X. Chen, H. Ü. Kaniskan and J. Jin, *J. Am. Chem. Soc.*, 2021, **143**, 15073–15083.
22 K. Moreau, M. Coen, A. X. Zhang, F. Pachl, M. P. Castaldi, G. Dahl, H. Boyd, C. Scott and P. Newham, *Br. J. Pharmacol.*, 2020, **177**, 1709–1718.
23 C. Steinebach, Y. L. D. Ng, I. Sosic, C.-S. Lee, S. Chen, S. Lindner, L. P. Vu, A. Bricelj, R. Haschemi, M. Monschke, E. Steinwarz, K. G. Wagner, G. Bendas, J. Luo, M. Gütschow and J. Krönke, *Chem. Sci.*, 2020, **11**, 3474–3486.
24 L. M. Gockel, V. Pfeifer, F. Baltes, R. D. Bachmaier, K. G. Wagner, G. Bendas, M. Gütschow, I. Sosič and C. Steinebach, *Arch. Pharm.*, 2022, DOI:10.1002/ardp.202100467.
25 T. Anastassiadis, S. W. Deacon, K. Devarajan, H. Ma and J. R. Peterson, *Nat. Biotechnol.*, 2011, **29**, 1039–1045.
26 M. Grasso, M. A. Estrada, C. Ventocilla, M. Samanta, J. Maksimoska, J. Villanueva, J. D. Winkler and R. Marmorstein, *ACS Chem. Biol.*, 2016, **11**, 2876–2888.
27 G. Bollag, P. Hirth, J. Tsai, J. Zhang, P. N. Ibrahim, H. Cho, W. Spevak, C. Zhang, Y. Zhang, G. Habets, E. A. Burton, B. Wong, G. Tsang, B. L. West, B. Powell, R. Shellooe, A. Marimuthu, H. Nguyen, K. Y. J. Zhang, D. R. Artis, J. Schlessinger, F. Su, B. Higgins, R. Iyer, K. D'Andrea, A. Koehler, M. Stumm, P. S. Lin, R. J. Lee, J. Grippo, I. Puzanov, K. B. Kim, A. Ribas, G. A. McArthur, J. A. Sosman, P. B. Chapman, K. T. Flaherty, X. Xu, K. L. Nathanson and K. Nolop, *Nature*, 2010, **467**, 596–599.
28 The X-ray crystallographic data collection of **3** was performed on a Bruker X8 –Kappa Apex-II diffractometer at 100(2) K. The diffractometer was equipped with a low-temperature device (Bruker Kryoflex I, Bruker AXS) and used Mo-Kα Radiation (λ=0.71073 Å). intensities were measured by fine-slicing ϕ- and ω-scans and corrected for background, polarization and lorentz effects. A semi-empirical absorption correction was applied for the data sets by using Bruker's SADABS program including a semi-empirical absorption correction according to Blessing's method. The structures were solved by intrinsic phasing methods and refined anisotropically by the least-squares procedure implemented in the ShelX-2014/7 program system.

View Article Online
DOI: 10.1039/D2MD00064D

The hydrogen atoms were included isotropically using a riding model on the bound carbon atoms. CCDC 2143596 contains the supplementary crystallographic data for this paper. These data are provided free of charge by the Cambridge Crystallographic Data Centre.

29 C. Steinebach, S. A. Voell, L. P. Vu, A. Bricelj, I. Sosič, G. Schnakenburg and M. Gütschow, *Synthesis*, 2020, **52**, 2521–2527.

30 C. Steinebach, H. Kehm, S. Lindner, L. P. Vu, S. Köpff, Á. López Mármol, C. Weiler, K. G. Wagner, M. Reichenzeller, J. Krönke and M. Gütschow, *Chem. Commun.*, 2019, **55**, 1821–1824.

31 C. Steinebach, I. Sosič, S. Lindner, A. Bricelj, F. Kohl, Y. L. D. Ng, M. Monschke, K. G. Wagner, J. Krönke and M. Gütschow, *Med. Chem. Commun.*, 2019, **10**, 1037–1041.

32 K. Lackey, M. Cory, R. Davis, S. V. Frye, P. A. Harris, R. N. Hunter, D. K. Jung, O. B. McDonald, R. W. McNutt, M. R. Peel, R. D. Rutkowske, J. M. Veal and E. R. Wood, *Bioorg. Med. Chem. Lett.*, 2000, **10**, 223–226.

33 M. S. Gadd, A. Testa, X. Lucas, K.-H. Chan, W. Chen, D. J. Lamont, M. Zengerle and A. Ciulli, *Nat. Chem. Biol.*, 2017, **13**, 514–521.

34 X. Han, C. Wang, C. Qin, W. Xiang, E. Fernandez-Salas, C.-Y. Yang, M. Wang, L. Zhao, T. Xu, K. Chinnaswamy, J. Delproposto, J. Stuckey and S. Wang, *J. Med. Chem.*, 2019, **62**, 941–964.